Food Chemistry 119 (2010) 703–714

Contents lists available at ScienceDirect

Food Chemistry

journal homepage: www.elsevier.com/locate/foodchem

Digestion stability and evaluation of the metabolism and transport of olive oil phenols in the human small-intestinal epithelial Caco-2/TC7 cell line

Aranzazu Soler [a], Maria P. Romero [a], Alba Macià [a], Shikha Saha [b], Caroline S.M. Furniss [b], Paul A. Kroon [b], Maria J. Motilva [a,*]

[a] *Food Technology Department, Escuela Técnica Superior de Ingeniería Agraria, Universidad de Lleida, Av/Alcalde Rovira Roure 191, 25198 Lleida, Spain*
[b] *Institute of Food Research, Norwich Research Park, Norwich NR4 7UA, UK*

ARTICLE INFO

Article history:
Received 12 March 2009
Received in revised form 19 May 2009
Accepted 7 July 2009

Keywords:
Phenols
Virgin olive oil
Metabolism
Digestibility
Caco-2 cells

ABSTRACT

The aims of this study were to investigate (i) the metabolism of olive oil phenolics by intestinal epithelial cells and (ii) their transport across epithelial cell monolayers. The various conjugates and derivatives produced by the intestinal epithelial cells were identified following separation by ultra-performance liquid chromatography (UPLC), using a combination of UV/visible spectra, mass spectrometry and specific enzyme treatments (β-glucuronidase and aryl-suphatase). Limited metabolism of olive oil phenolics was observed using Caco-2/Tc7 cells as a model of the human intestinal epithelium, and the methylated conjugates were the major metabolites detected. The results of the transport rate data for phenols and their metabolites to the apical, cellular, and basolateral compartments after apical loading of the phenol at 100 μM showed a time-dependent efflux of various free and conjugated forms of phenols.

1. Introduction

The beneficial effects of a Mediterranean diet on human health are widely known and it is commonly considered that the presence of a variety of antioxidant-rich foods in such diets is at least partly responsible. Virgin olive oil represents the principal fat component of the Mediterranean diet and it is a source of at least 30 phenolic compounds. The most important phenolic compounds that have been identified in olive oil are phenolic alcohols (such as hydroxytyrosol and tyrosol), secoiridoid derivatives (such as the dialdehydic form of elenolic acid linked to tyrosol (*p*-HPEA-EDA), the aldehydic form of elenolic acid linked to tyrosol (*p*-HPEA-EA), the dialdehydic form of elenolic acid linked to hydroxytyrosol (3,4-DHPEA-EDA), 4-(acetoxyethyl)-1,2-dihydroxybenzene (3,4-DHPEA-AC), oleuropein aglycone (3,4-DHPEA-EA) and its methylated form (methyl 3,4-DHPEA-EA)), phenolic acids and derivatives (such as vanillic acid and vanillin, respectively), lignans (pinoresinol and acetoxypinoresinol) and flavonoids (including luteolin and apigenin) (Bendini et al., 2007).

Phenolic compounds are of fundamental importance in virgin olive oil for their nutritional properties, sensory characteristics, and the shelf life of the product (Morelló, Motilva, Tovar, & Romero, 2004; Servili et al., 2008). In particular, the phenolic compounds are potent antioxidants, and can confer a marked bitter taste or a sweet taste typical of some virgin olive oil (Artajo, Romero, Morelló, & Motilva, 2006; Esti, Contini, Moneta, & Sinesio, 2009). In addition, they are thought to play an important role in human diets as preventative agents against several diseases (Owen et al., 2000, 2004).

In experimental studies, olive oil phenolics have been shown to: (1) be powerful antioxidants, more potent than vitamin E in preventing lipids and DNA oxidation (Fitó et al., 2000; Masella et al., 2004); (2) prevent endothelial dysfunction by decreasing the expression of cell adhesion molecules (Carluccio et al., 2003), increasing nitric oxide (NO) production by increasing endothelial NO synthase activity (Moreno, 2003) and quenching vascular endothelium intracellular free radicals (Massaro et al., 2002); (3) inhibit platelet-induced aggregation (Petroni et al., 1995); and (4) enhance transcription of the antioxidant enzyme glutathione peroxidase (GSH-Px) (Masella et al., 2004). Recently, an ibuprofen-like activity has been described for oleocanthal or *p*-HPEA-EDA, a ligstroside aglycone present in olive oil (Beauchamp et al., 2005). Other potential activities of olive oil phenolic compounds include chemopreventive activity (Owen et al., 2004).

Nevertheless, to achieve any effect in a specific tissue or organ, these bioactive compounds must be bioavailable, which refers to the compound's tendency to be extracted from the food matrix, and they must then be absorbed from the gut *via* the intestinal cells. Experimental results from *in vitro* cellular systems have shown that hydroxytyrosol is quantitatively transported into the small-intestinal epithelial cells by passive diffusion (Manna et al.,

* Corresponding author. Tel.: +34 973 702817; fax: +34 973 702596.
E-mail address: motilva@tecal.udl.es (M.J. Motilva).

0308-8146/$ - see front matter © 2009 Elsevier Ltd. All rights reserved.
doi:10.1016/j.foodchem.2009.07.017

2000). Data from *in vivo* experiments with animals and humans have confirmed that olive oil phenolics are well absorbed at the intestinal level (Tuck, Freeman, Hayball, Stretch, & Stupans, 2001). Tyrosol and hydroxytyrosol are absorbed by humans in a dose-dependent manner (i.e., the olive oils with the highest concentration of phenolics deliver the highest concentrations of hydroxytyrosol to blood) (Visioli et al., 2000). Even from moderate doses (25 ml/day), which are lower than the traditional daily dietary intake in Mediterranean countries (Visioli et al., 2003), it has been shown that around 98% of these phenolics are present in plasma and urine in conjugated forms, mainly glucurono-conjugates. These observations indicate that the first-pass intestinal/hepatic metabolism of the ingested phenolics is extensive (Marrugat et al., 2004).

However, data regarding the metabolism of olive oil phenolics in the human body are very limited, and contrasting results have been obtained regarding the amounts and forms in which they are present in plasma and excreted in urine (Miró-Casas et al., 2003). A first step would be trying to know the fate of olive oil phenolic compounds during the digestion, metabolism and absorption processes, how rapidly they are released from the food matrix under the physiological conditions occurring *in vivo*, and the stability of these compounds under these conditions.

The studies of bioavailability of phytochemicals carried out in animals or human subjects are complex, expensive and lengthy. In this sense, *in vitro* digestion models permit the characterisation of phenolics during digestion under physiological conditions, caused by alimentary enzymes, and to obtain information going beyond that gained by the chemical analysis of food. Furthermore, the *in vitro* digestion models allow the screening of multiple samples and may provide data on the relative bioavailability of different polyphenolic components. In combination with a cultured cell model that facilitates studies of small-intestinal absorption and metabolism, it is possible to determine the relationship between the molecular structures, gastrointestinal stability, conjugation and extent of absorption for virgin olive oil phenols as an important step towards elucidating the potential impact of these compounds on human health.

The first objective of the present study was to evaluate the digestive stability of phenols from virgin olive oil, using an *in vitro* gastrointestinal digestion method simulating gastric and small-intestinal phases. The second part of the study was focused on investigating (i) the metabolism of olive oil phenolics by intestinal epithelial cells and (ii) their transport across epithelial cell monolayers using a Caco-2/TC7 cell culture model. For the second objective, the most representative components of the phenolic fraction of virgin olive oil that were transferred to the aqueous fraction during the simulated digestion were selected for investigation.

2. Materials and methods

2.1. Phenol standards

Hydroxytyrosol, tyrosol, *p*-coumaric acid, and luteolin were purchased from Extrasynthèse (Genay, France). (+)-Pinoresinol was acquired from Arbo Nova (Turku, Finland).

2.2. In vitro digestion model

Triplicate samples of virgin olive oil were digested. The procedure was adapted from the method outlined by Gil-Izquierdo, Zafrilla, and Tomás-Barberán (2002), slightly modified. The method consists of two sequential steps; an initial pepsin/HCl digestion for 2 h at 37 °C, to simulate gastric conditions, followed by a digestion with bile salts/pancreatin for 2 h at 37 °C to simulate duodenal digestion. For the pepsin/HCl digestion, a sample of olive oil (15 g) was mixed with pepsin (14,800 U) in 20 ml of water acidified with HCl to reach pH 2 and was then incubated in a 37 °C orbital shaker (250 rpm) (Infors AG CH-4103, Bottmingen, Switzerland) for 2 h. After gastric digestion, the pancreatic digestion was simulated. The pH was increased to 6.5 with $NaHCO_3$ (0.5 N) and then 5 ml (1:1; v/v) of pancreatin (8 mg/ml)–bile salt (50 mg/ml) were added and incubated in a 37 °C shaking orbital (250 rpm) for 2 h.

After each step of digestion, lipid (oil digesta) and water (aqueous micellar) phases were separated by ultracentrifugation at 30,000*g* for 20 min at 4 °C. The phenols present in both phases from the pepsin–HCl and pancreatin–bile digestions were extracted and analysed by liquid chromatography-tandem mass spectrometry, as described by Suárez, Macià, Romero, and Motilva (2008).

2.3. Maintenance of the Caco-2/TC7 cell line

The manipulation of the cell line was carried out in an Envair Class II model safety cabinet with laminar flow. Aseptic techniques were used to ensure the sterility of cells and growing medium, so all glassware was sterilised in an autoclave, consumables were packaged and sterilised or pre-sterilised also in the autoclave and water was purified using a Millipore filtration unit (Millipore Corporation, Billerica, MA) and was subsequently sterilised in an autoclave. Both the media and the solutions were pre-warmed at 37 °C before they established contact with the cells.

The Caco-2/TC7 cells were used between passages 51 and 61 in the metabolism experiments and between 49 and 51 for transport experiments. Cells were grown in 75 cm^2 flasks, maintained in DMEM+ at 37 °C with 5% CO_2 and 95% air, and new flasks were seeded at a concentration of 2–4 $\times$ 10^4 cells/cm^2.

2.4. Metabolism experiments

2.4.1. Olive oil phenols cellular metabolism experiments

Caco-2/TC7 cells were seeded at 2–4 $\times$ 10^4 cells/cm^2 on six-well plates. All metabolic experiments were carried out in triplicate, such that two six-well plates were required per compound. Three of the 12 wells were not seeded with cells for use as a control that would contain only medium and phenolic compound. The medium was changed every 2nd day, and the cells were allowed to grow and differentiate up to 7 days after reaching confluence. At this point the medium was aspirated and cells were washed three times with phosphate-buffered saline (PBS). Phenols dissolved in methanol (final methanol concentration in the medium = 0.04%) were added to the media of treatment cells at a final concentration of 40, 50 and 100 μM, and to control cells a solution of the same volume and concentration of HPLC-grade methanol was added. Control and treated cells were incubated at 37 °C, for 1, 6 or 24 h. The medium also contained ascorbic acid (100 μM) as a protective antioxidant. After incubation, the culture medium was split into two aliquots of 1 ml in Eppendorf vials and methanol (25 μl) and glacial acetic acid (25 μl) were added. The cells were washed three times with PBS and then harvested by scraping after addition of water (400 μl), methanol (25 μl) and glacial acetic acid (50 μl). For all samples, galangin (50 μM final concentration) was added as an internal standard. All samples were kept frozen at −20 °C until phenolic analysis.

On the day of the phenolic analysis, medium and cell samples were thawed if necessary, mixed on a bench-top vortex mixer, and centrifuged for 10 min at 13,000 rpm at 4 °C in a bench-top micro-centrifuge and the supernatant removed and placed in an HPLC vial for analysis. Cell samples were sonicated for 10 min at room temperature to break down the cell membrane before centrifugation.

The results of the metabolism experiments were expressed as total nmols in culture media or cells after the incubation. Additionally, the metabolism yield is expressed as the percentage of the molar amount transformed for each phenol in relation to the initial concentration in the culture media (40 μM = 80 nmol; 100 μM = 200 nmol; 50 μM = 100 nmol).

2.4.2. Enzymatic hydrolysis of potential metabolites

A fraction of the medium from cell incubations was subjected to an enzymatic hydrolysis prior to HPLC analysis. For that purpose, media samples (1 ml) were treated with 23 mg (150 U) of β-glucuronidase, or with 10 mg (150 U) of aryl-suphatase (Sigma–Aldrich, Poole, UK) or with both enzymes simultaneously. The hydrolysis solutions were shaken for a minute to disperse the enzymes and incubated at 37 °C for 2 h prior to preparation for phenol analysis as indicated above.

2.5. Transport experiments

2.5.1. Evaluation of monolayer integrity in transwells

(i) *Measuring the trans-epithelial electrical resistance (TEER)*: The TEER of the Transwells was routinely measured directly before the change of culture medium. A Millicell-ERS volt ohmmeter (Millipore Corporation), was used to take the measurements as per the supplied instructions. The TEER was expressed in $\Omega\,cm^2$ after subtracting the reading of the resistance of the supporting filter (well without monolayer of cells) and multiplying it by the area of the monolayer (1.1 cm^2). The monolayer was considered to be sufficiently integrated if the TEER was greater than 180 $\Omega\,cm^2$.

(ii) *Phenol red transport*: The culture medium was removed from apical and basolateral compartments and both areas were washed three times with PBS. After this, 0.6 ml of DMEM+ medium containing phenol red was added to the apical compartment, while the basolateral compartment was loaded with 1.5 ml DMEM+ without phenol red. Cells were incubated at 37 °C for 60 min and then the diffusion of phenol red across the monolayer from the apical compartment to the lower basolateral was determined by measuring absorbance at 479 nm. Wells that supported <0.1% of phenol red transport under these conditions were considered suitable for use.

2.5.2. Determination of trans-epithelial transport

First, the medium was aspirated from both apical and basolateral compartments and the cells were washed three times with PBS.

For 9 of the 12 wells, medium (0.6 ml) containing 100 μM ascorbic acid was added to the apical compartment and the phenolic added at the appropriate concentration. To the other three wells, medium containing ascorbic acid and methanol (vehicle) was added to serve as a control. The basolateral compartment of all 12 wells was filled with 1.5 ml of DMEM containing 100 μM ascorbic acid. Plates were incubated at 37 °C, for 1, 6 and 24 h (three wells per time period). Following incubation, apical medium (0.6 ml), basolateral medium (1.5 ml) and cells (collected by adding 400 μl of water and scraping the monolayer after washing the cells three times with PBS) were placed in clean Eppendorf tubes. Methanol (25, 50 and 25 μl) and glacial acetic acid (25, 50 and 50 μl) were added to the apical medium, basolateral medium and cell samples, respectively. Galangin (final concentration 50 μM) was added to all samples as an internal standard and samples were frozen until analysis. Prior to analysis the samples were thawed, mixed on a bench-top vortex mixer, and centrifuged for 10 min at 13,000 rpm at 4 °C. Before centrifugation, suspension cells were sonicated for 10 min at room temperature to break down the cell membrane and the supernatant was analysed. The results of transport experiments were expressed as relative transport rate in the apical, cellular and basolateral compartments.

2.6. Phenolic analysis by UPLC-MS

The analyses were performed by UPLC-PDA-MS, as described by Suárez et al. (2008). Ionisation was achieved using an electrospray (ESI) interface operating in the negative mode $[M-H]^-$. Mass spectra in the full-scan mode were collected by scanning between m/z 80 and 800, and the most abundant ions for each phenolic compound were monitored by selected ion monitoring (SIM) acquisition. The ionisation source parameters were similar to those described by Suárez et al. (2008).

2.7. Phenolic metabolites characterisation and quantification

Due to the absence of pure standards, the phenolic metabolites produced were quantified on the basis of the response factors for the corresponding parent compounds. The mass spectrometer was managed in the full-scan and the SIM modes simultaneously. In order to characterise and identify their structures, full-scan mode at different cone voltages (from 20 to 60 V) was used. First, a low cone voltage was applied to determine the pseudomolecular ion $[M-H]^-$. Then, in order to obtain further structural information, high cone voltages were applied and specific fragment ions were generated. As we wanted to detect the phenolic metabolites at low concentrations, the SIM mode was used for the quantification because in the scan mode there was no response at these levels of concentration.

3. Results and discussion

3.1. Phenol digestion stability

The impact of both gastric and small-intestinal phases of digestion on olive oil phenols was examined. The extent of digestion was evaluated by quantifying the phenolics in both the lipid (oil digesta) and water (aqueous micellar) phases, calculated back to a 1 g sample of the virgin olive oil test food (Table 1). All the major olive oil phenolics (tyrosol, hydroxytyrosol and the related secoiridoid structures (3,4-DHPEA-EDA and *p*-HPEA-EDA) and elenolic acid) showed good stability in the gastric digestion model. Although the profile of phenolics was similar in the oil digesta and aqueous micellar phases, the relative distribution between the phases was different for each of the phenolic compounds. The amphiphilic characteristics of the secoiridoids permit their partition between the oily phase and the water phase, and they tended to be more concentrated in the aqueous phase because of their polar functional groups. On the other hand, the more hydrophobic flavonoids (apigenin and luteolin) were mainly present in the oily phase after gastric digestion.

The resistance of these phenol structures to the acid conditions of the stomach may be related with the conditions they have encountered during the oil extraction process. Indeed, the major forms of phenolics in the olive fruits are glycosides, and the aglycones (oleuropein, ligstroside, flavonoids and lignans) that are the predominant forms of phenolics in the olive oil are formed as a consequence of the acidic conditions and the presence of β-glucosidase activity when the olives are pasted during olive oil

Table 1
Relative amounts of phenols in test oil, digesta and aqueous micellar fraction after *in vitro* digestion of virgin olive oil (VOO). The results are expressed as total nmol of phenol in each phase per gram of virgin olive oil digested.

Phenol	Test oil (nmol/g VOO)	Gastric digestion		Duodenal digestion	
		Oil digesta (nmol)	Aqueous micellar (nmol)	Oil digesta (nmol)	Aqueous micellar (nmol)
Hydroxytyrosol	19.9	2.88	32.8	0.64	26.1
Tyrosol	15.3	3.68	27.9	4.16	48.6
p-Coumaric acid	0.85	0.44	0.25	0.00	0.00
Elenolic acid	207	59.3	194	0.61	2.43
3,4-DHPEA-EDA	384	22.2	236	0.00	1.72
p-HPEA-EDA	39.4	9.85	21.7	0.00	0.00
Pinoresinol	4.62	12.1	0.00	9.64	0.00
(+)-1-Acetoxypinoresinol	28.9	17.8	22.8	26.9	24.1
Apigenin	3.59	3.50	0.00	1.21	0.00
Luteolin	11.5	10.0	0.36	0.60	3.67

production (Bendini et al., 2007). Moreover, the resistance of olive oil phenolics to acidic gastric conditions may explain the increase in concentration of plasma tyrosol, hydroxytyrosol, and 3-*O*-methylhydroxytyrosol at 60 min after the intake of olive oil with high phenolic content (Ruano et al., 2007).

In contrast, the stability of these dietary phenols when exposed to small-intestinal conditions (incubation at pH 6.5 with pancreatin and bile salts at 37 °C for 2 h) was very low (Table 1). In fact, of the main phenols of virgin olive oil, only 10% of the secoridoids 3,4-DHPEA-EDA and *p*-HPEA-EDA, were recovered in the aqueous phase. The flavonoids were also unstable, but these phenolics were mainly recovered from the oil digesta fraction. In contrast, lignans were quite stable to gastrointestinal and duodenal digestion conditions.

In addition to determining their stability under gastric and duodenal digestion conditions, the potential bioavailability of some olive oil phenolics transferred to the aqueous phase after the duodenal digestion was determined. It is known that the rate at which phenolics are taken up by enterocytes from aqueous environments (the first step in absorption) is dependent on their concentration in solution. Therefore, the concentration of phenolic in solution is an important factor in determining bioavailability because the phenolics can be considered bioavailable. However, it is necessary to remember that the digested aqueous phase almost certainly contains micelles and therefore will include phenolic components that are not truly in solution, but associated with these hydrophobic-centred micelles. It is not currently known whether micelle-borne phenolics are more or less bioavailable for intestinal uptake.

Having determined the extent to which olive oil phenolics are released to the aqueous phase during gastro-duodenal digestion, it was next necessary to measure the relative rates of uptake and trans-epithelial transport of the phenolics by intestinal epithelial cells.

3.2. Detection and identification of phenol metabolites by differentiated Caco-2/TC7 Cells

The intestinal metabolism of the major virgin olive oil phenols quantified in the aqueous duodenal phase (Table 1) (tyrosol, hydroxytyrosol, and luteolin) was studied following application at different concentrations (40, 50 and 100 μM) for different incubation periods (1, 6 and 24 h), using differentiated Caco-2/TC7 cell monolayers as a model of the human intestinal epithelium. As consequence of the lack of commercial standards, *p*-coumaric acid and pinoresinol were used instead of elenolic acid and acetoxypinoresinol, respectively. The human colon adenocarcinoma cell line TC7 corresponds to a spontaneously differentiating clone derived from the original Caco-2 cell population (Chantret et al., 1994). The main advantage of this cellular line is related with its stability when grown as monolayers on Transwell inserts in relation to the parental Caco-2 parent cell line.

Table 2
Chromatographic and mass characteristics of hydroxytyrosol (1), tyrosol (2), *p*-coumaric acid (3), pinoresinol (4) and luteolin (5) and the metabolites (M) formed after incubation using differentiated Caco-2/Tc7 cells monolayer as a model of the human intestinal epithelium.

Peak	MW[a]	RT[b] (min)	Comparison to standard	$[M-H]^-$	Fragment ions	Reaction to (G) or (S)[c]	Proposed compound
1	154	2.24	Available	153	123	–	Hydroxytyrosol
M1	234	7.11	Not available	233	153, 123	S	Hydroxytyrosol sulphate
M2	248	8.36, 9.50	Not available	247	233, 167, 153, 123	S	Hydroxytyrosol methyl- sulphate
M3	168	8.96	Not available	167	153, 123	–	Hydroxytyrosol methyl
2	138	3.34	Available	137	119	–	Tyrosol
M4	152	4.80	Not available	151	137, 119	–	Tyrosol methyl
M5	218	8.40	Not available	217	137, 119	S	Tyrosol sulphate
3	164	7.40	Available	163	119	–	Coumaric acid
M6	324	7.80	Not available	323	163, 119	S	Coumaric acid di sulphate
M7	178	15.06	Not available	177	145, 119	–	Coumaric acid methyl
4	358	16.34	Available	357	212, 151, 117		Pinoresinol
M8	438	13.09	Not available	437	357, 151	S	Pinoresinol sulphate
M9	534	14.00	Not available	533	357, 151	G	Pinoresinol glucuronide
5	286	15.01	Available	285	212, 119	–	Luteolin
M10	462	13.5	Not available	461	285	G	Luteolin glucuronide
M11	300	16.65	Not available	299	285	–	Luteolin methyl
M12	476	17.60	Not available	475	461, 299, 285	G	Luteolin methyl-glucuronide

[a] Molecular weight (MW).
[b] Retention time (RT).
[c] (G): β-Glucuronidase, (S): aryl-sulfatase.

Cells were grown on dishes, and the metabolites were determined in the medium and in the cell. After the incubation, the resulting putative metabolites of the phenols produced by the intestinal epithelial cells were detected and identified following separation by UPLC using a combination of UV/visible spectra and mass spectrometry. Additionally confirmation of the conjugation

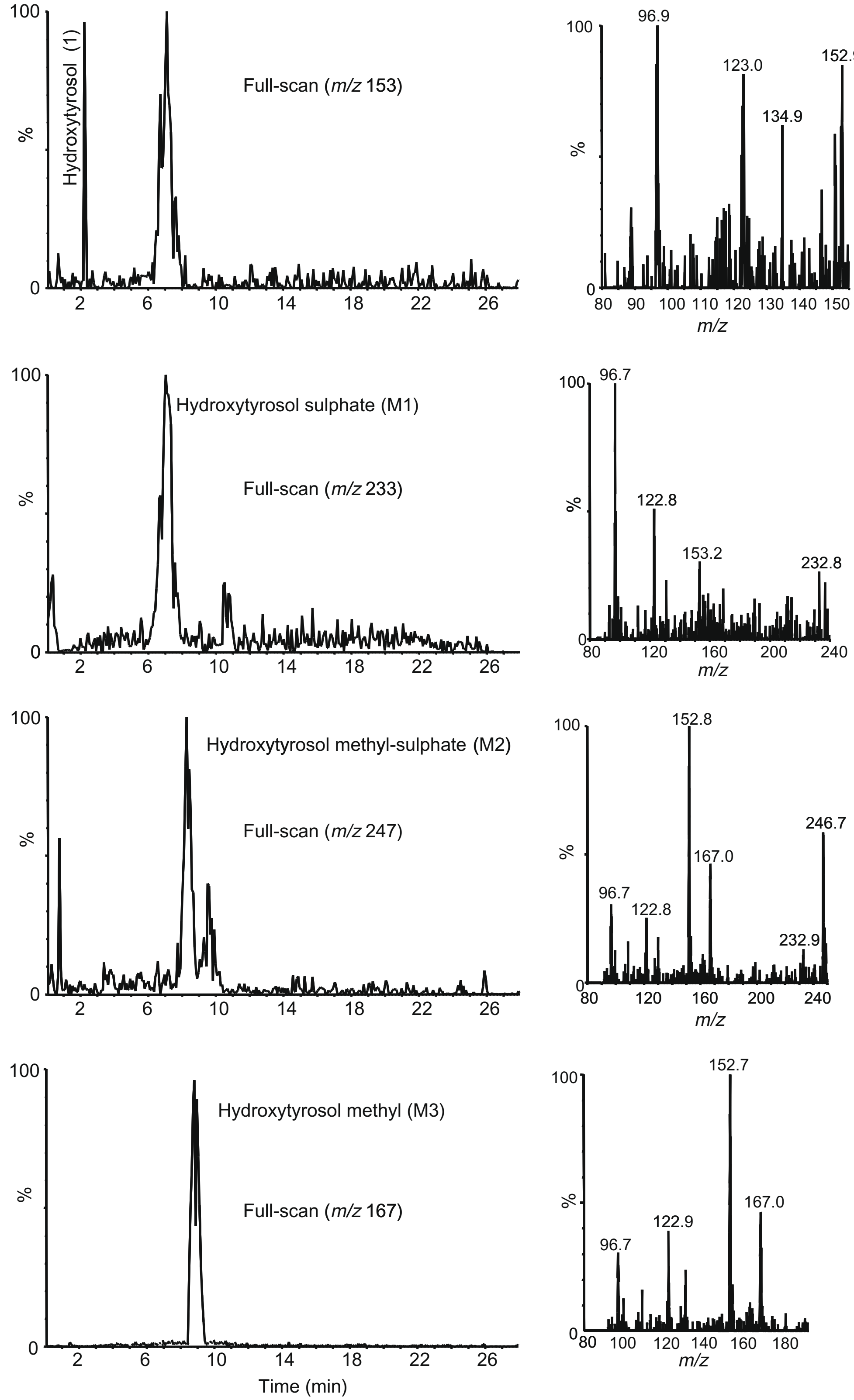

Fig. 1. Extracted ion chromatogram and the ESI-MS spectra of the native form of hydroxytyrosol and the generated metabolites: hydroxytyrosol sulphate (M1), hydroxytyrosol methyl-sulphate (M2) and hydroxytyrosol-methyl (M3).

was obtained by treatment of the medium samples with specific enzymes, β-glucuronidase and aryl-suphatase, resulting in the disappearance of the respective conjugates.

The native forms were identified by comparing the ESI-MS spectra of media/cell samples in full-scan mode and their retention time with those of pure standards. The various metabolites formed after incubation of the phenolic compounds with the cells were identified using ESI-MS spectra with additional information provided by specific enzymatic hydrolyses, i.e., with β-glucuronidase and aryl-suphatase. Table 2 shows chromatographic and mass characteristics of hydroxytyrosol, tyrosol, *p*-coumaric acid, pinoresinol and luteolin and their metabolites, and the reaction to the β-glucuronidase and aryl-suphatase treatments. Figs. 1–5 show the extracted ion chromatograms and the ESI-MS spectra of the native forms and the respective metabolites of hydroxytyrosol, tyrosol, *p*-coumaric acid, pinoresinol and luteolin, respectively.

Hydroxytyrosol (Fig. 1): Hydroxytyrosol was identified on the basis that the putative peak gave rise to the pseudomolecular ion $[M-H]^-$ at *m/z* 153 and the ion fragments at *m/z* 135 and 123. These fragment ions are due to the loss of a water molecule and the CH_2OH group, respectively. The ESI-MS spectrum of the compound that eluted at 7.11 min showed an intense ion at *m/z* 233, which formed two major fragment ions, one at *m/z* 153 and the other at *m/z* 123. These ions could be related to the loss of the sulphate molecule and the hydroxytyrosol rupture, respectively, and this evidence allowed putative identification of the metabolite as hydroxytyrosol sulphate (M1). At retention times of 8.36 and 9.50 min, another hydroxytyrosol metabolite was observed by examination of the ESI-MS spectra and it was characterised by an intense ion at *m/z* 247. The presence of the two peaks could be attributed to structural isomers. This metabolite presents a fragment ion at *m/z* 233 which can be explained by the loss of the methyl group, and a fragment at *m/z* 167 which can be described by the loss of the sulphate molecule. Therefore, this metabolite could be identified as hydroxytyrosol methyl-sulphate (M2). The metabolite hydroxytyrosol methyl (M3), gave the pseudomolecular ion $[M-H]^-$ at *m/z* 167 and the fragment ion at *m/z* 153, due to the loss of the methyl group.

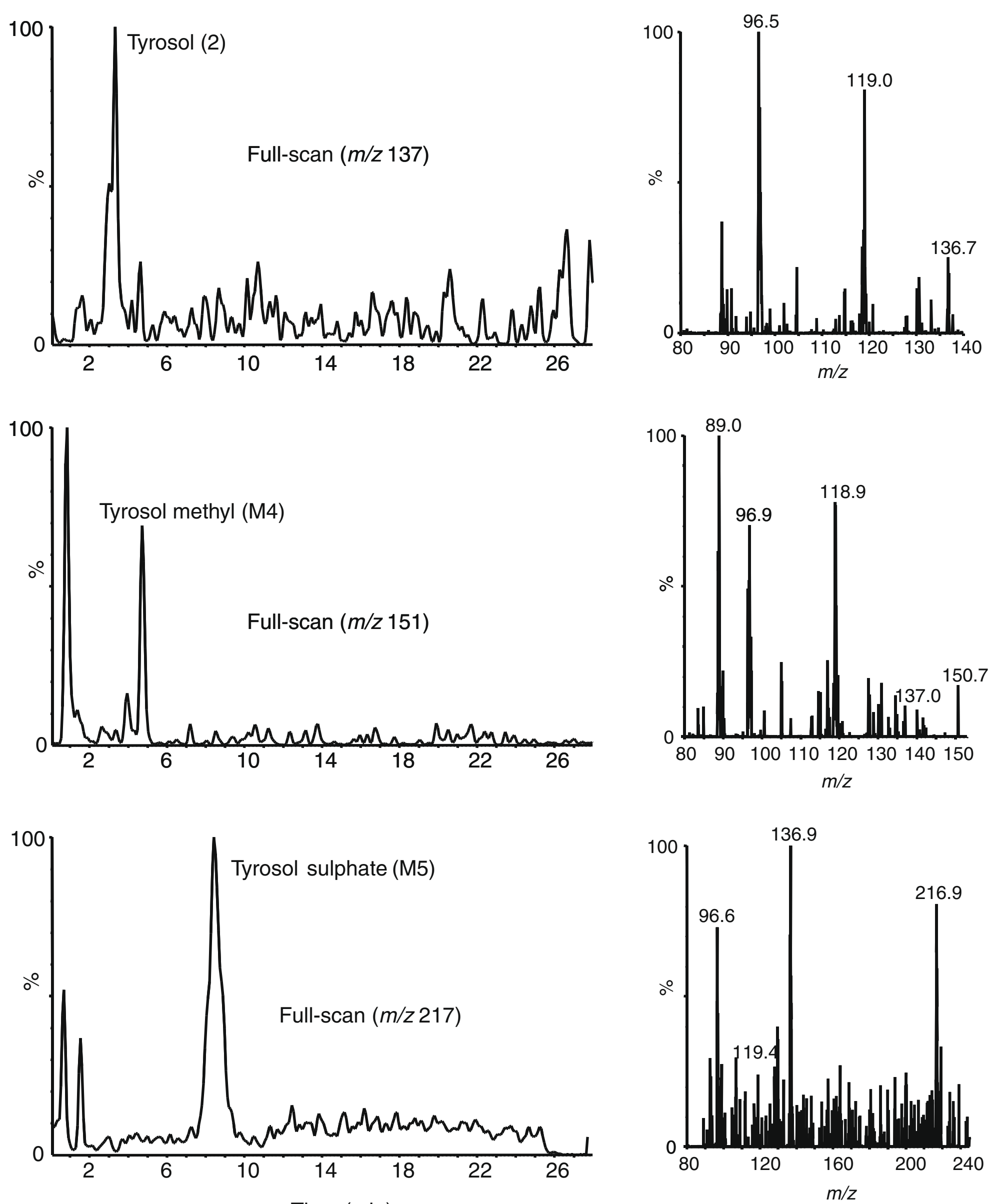

Fig. 2. Extracted ion chromatogram and the ESI-MS spectra of the native form of tyrosol and the generated metabolites: tyrosol-methyl (M4) and tyrosol sulphate (M5).

Tyrosol (Fig. 2): The spectrum generated for this compound gave the pseudomolecular ion $[M-H]^-$ at m/z 137 and a ion fragment at m/z 119. M4 and M5 are tyrosol metabolites, indicated by the production of fragment ions at m/z 137, which demonstrates the existence of the tyrosol molecule. The first metabolite (M4) gave the pseudomolecular $[M-H]^-$ at m/z 151 and the second one (M5) at m/z 217, which can be explained by the loss of the methyl group and the sulphate molecule, respectively.

p-Coumaric acid (Fig. 3): The spectrum generated for this compound gave the pseudomolecular $[M-H]^-$ at m/z 163. The fragment ion at m/z 119 is due to the loss of the carboxylic group (CO_2). M6 and M7 are coumaric acid metabolites by the fact that their fragment ion spectra include ions at m/z 163, which demonstrates the existence of the coumaric acid molecule and the additional fragment ion at m/z 119. The fragment m/z 145 is consistent with the loss of a water molecule. M6 was putatively identified as coumaric acid disulphate (evidence for the loss of two sulphate molecules). M7 was putatively identified as *p*-coumaric acid methyl (loss of methyl group on fragmentation).

Pinoresinol (Fig. 4): The spectrum generated for this compound gave the pseudomolecular molecule $[M-H]^-$ at m/z 357. M8 and M9 are pinoresinol metabolites on the basis that their fragments produce ions at m/z 357, which demonstrates the existence of the pinoresinol molecule. The first one (M8) gave the pseudomolecular $[M-H]^-$ at m/z 437 and the second one (M9) at m/z 533, which can be explained by the loss of the sulphate and the glucuronide molecule, respectively.

Luteolin (Fig. 5): The spectrum generated for this compound gave the pseudomolecular ion $[M-H]^-$ at m/z 285. As can be seen in Table 1, four metabolites could be identified (M10, M11, M12 and M13) by the fact that their fragment ions produce ions at m/z 285, which demonstrates the existence of the luteolin molecule. M10 and M11 could be identified as luteolin monoglucuronides ($[M-H]^- = m/z$ 461) and luteolin methyl ($[M-H]^- = m/z$ 299) due to the loss of glucuronide molecule and the methyl group, respectively. M12 showed fragment ions at m/z 461 and 299 and M12 was tentatively identified as luteolin methyl-monoglucuronide ($[M-H]^- = m/z$ 475). The last luteolin metabolite identified could

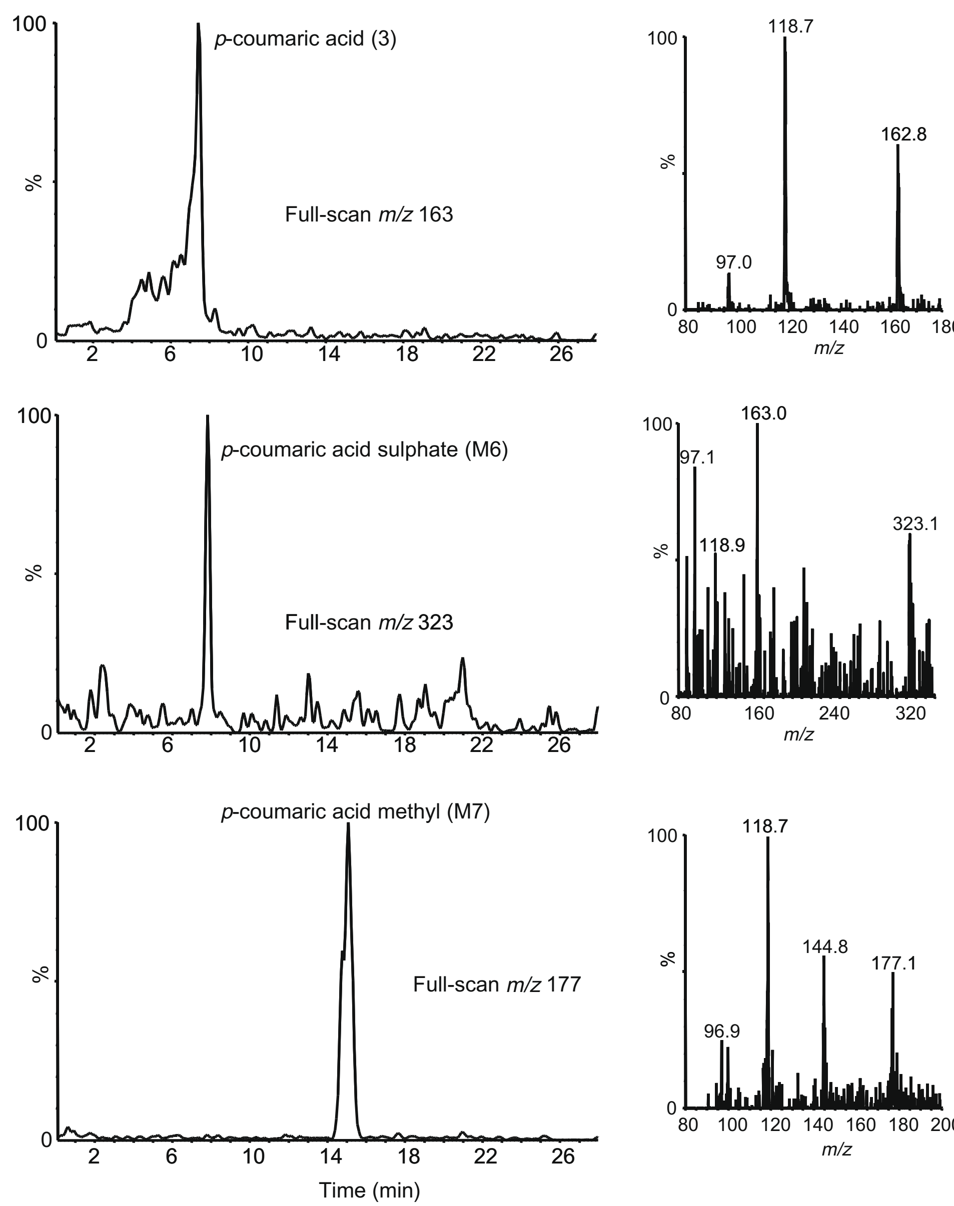

Fig. 3. Extracted ion chromatogram and the ESI-MS spectra of the native form of *p*-coumaric acid and the generated metabolites: *p*-coumaric acid sulphate (M6) and *p*-coumaric acid-methyl (M7).

be luteolin dimethyl ($[M-H]^- = m/z$ 313) the fragment ions of which were m/z 299 and m/z 285. These could be explained by the loss of a single methyl group and two methyl groups, respectively.

The phenolic compounds and their metabolites were quantified (or tentatively quantified with respect to metabolites) in the SIM mode, because it has the advantage of increasing sensitivity in addition to reducing noise from interfering compounds.

3.3. Quantification of metabolites and metabolism yield

As a consequence of the low conjugate production observed after 1 h of incubation, it was decided to increase the initial concentration of the different phenols from 40 to 100 μM taking account of the different incubation times. Epithelial cell metabolism of phenolic compounds was monitored at 1-, 6- and 24-h incubation times, analysing the products formed as a consequence of cell metabolism in the extracellular culture medium as well as in cytoplasmatic contents after cell lysis (Table 3). The metabolites present in the medium could have been produced intracellularly and excreted to the apical side of the monolayer or produced directly in the medium by secreted enzymes. The concentrations of the phenols after incubation in the Caco-2/TC7 cell monolayer were expressed as nmol present in the total volume of culture medium or cells. Additionally, the metabolism yield was expressed as the percentage of transformed phenol in relation to its initial concentration in the cellular medium.

A previous study by Manna et al. (2000) focusing on molecular transport, using differentiated Caco-2 cell monolayers. demonstrated that hydroxytyrosol transport occurred *via* a passive bidirectional diffusion mechanism. The only hydroxytyrosol metabolite, with a 10% conversion, detectable in the culture

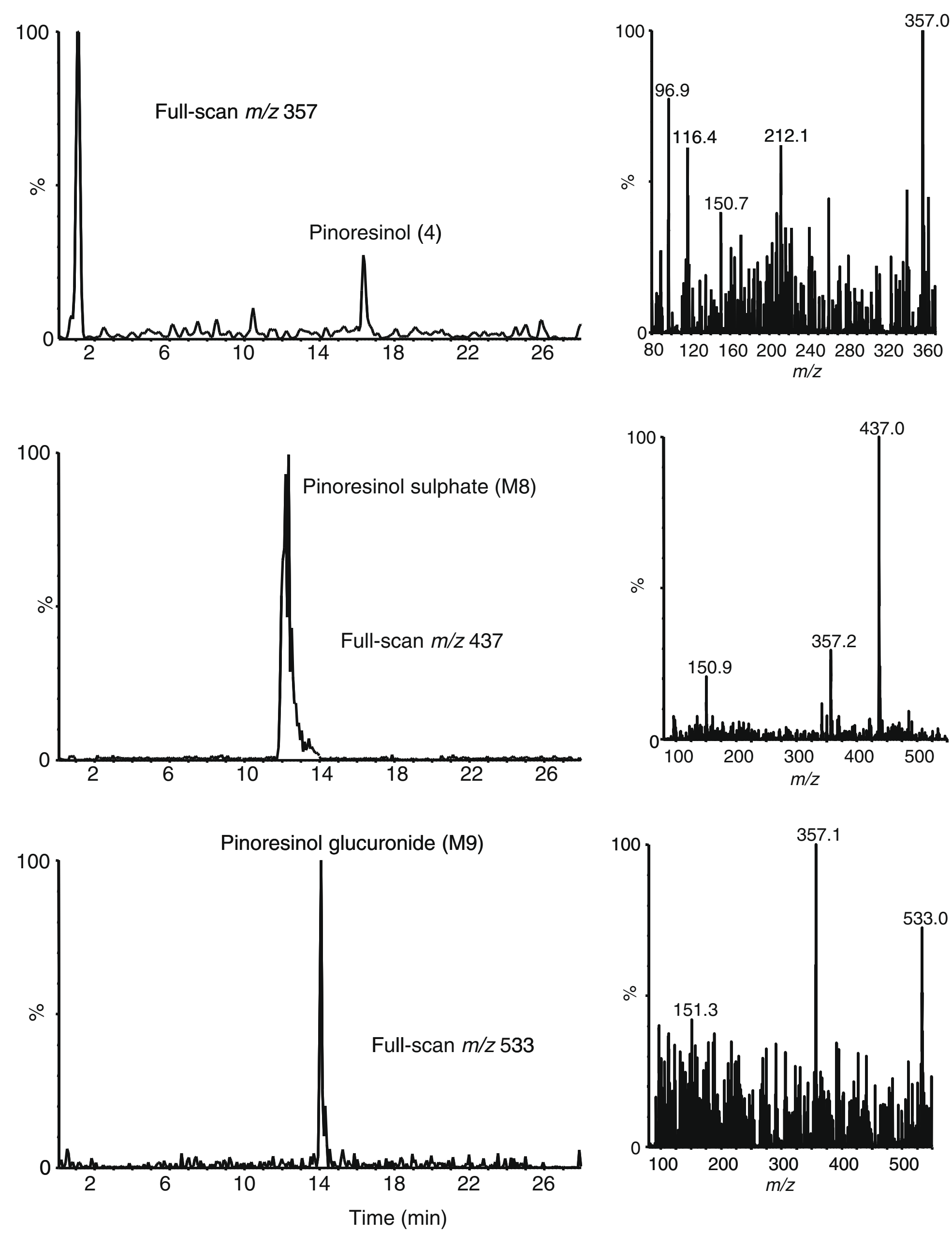

Fig. 4. Extracted ion chromatogram and the ESI-MS spectra of the native form of pinoresinol and the generated metabolites: pinoresinol-sulphate (M8) and pinoresinol-glucuronide (M9).

medium was 3-hydroxy-4-methoxyphenylethanol, the product of catechol-*O*-methyltransferase activity. In keeping with these earlier findings, in the present study the highest metabolism yield corresponded with the formation of methyl hydroxytyrosol, ranging from 10.7% to 18.6%, dependent on the incubation period. In addition, small quantities of sulphated and methyl-sulphated conjugates of hydroxytyrosol were also formed after the 6 and 24 h of incubation. The major metabolism of hydroxytyrosol observed in our study could be related to a better conjugation efficacy of the Caco-2/TC7 compared with the parental Caco-2 cell line that was

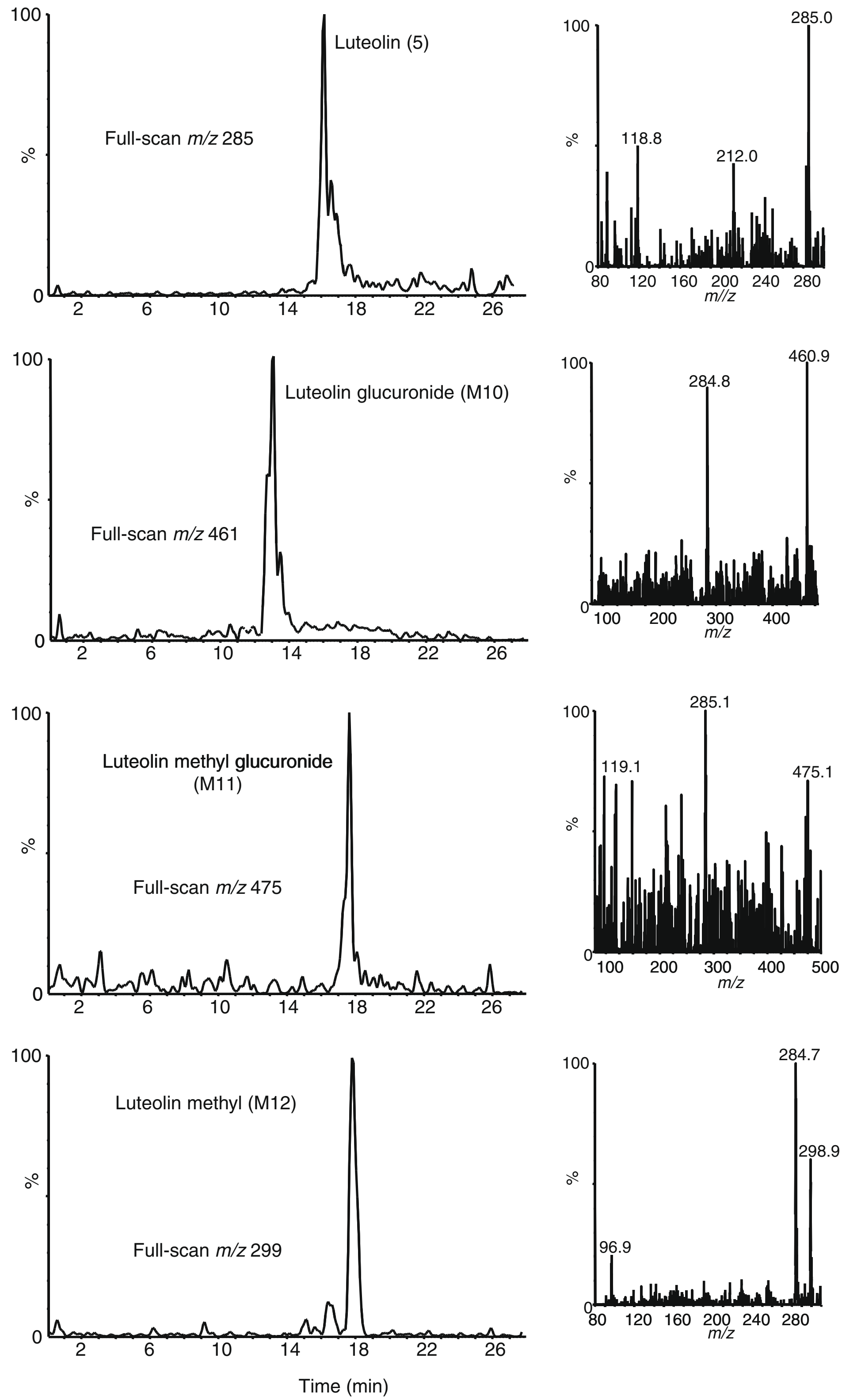

Fig. 5. Extracted ion chromatogram and the ESI-MS spectra of the native form of luteolin and the generated metabolites: luteolin-glucuronide (M10), luteolin-methyl (M11) and luteolin-methyl-glucuronide (M12).

Table 3
Amounts of various phenols and their metabolites (expressed as nmol/2 ml culture medium) in cell culture medium and cells after incubation at different concentrations in the culture medium (40 μM = 80 nmol; 100 μM = 200 nmol; 50 μM = 100 nmol) and incubation periods, using differentiated Caco-2/Tc7 cell monolayers as a model of the human small-intestinal epithelium. The metabolism yield is expressed as percentage of the nmol transformed of each phenol.

Phenols and metabolites	Amount in cell culture medium (nmol)			Amount in cells (nmol)		
	40 μM[a], 1 h	100 μM[b], 6 h	50 μM[c], 24 h	40 μM[a], 1 h	100 μM[b], 6 h	50 μM[c], 24 h
Hydroxytyrosol	18.1	126	30.1	7.28	n.d.	n.d.
Hydroxytyrosol methyl	8.58 (10.7%)	28.8 (14.4%)	18.6 (18.6%)	n.d.	29.8 (14.9%)	n.d.
Hydroxytyrosol sulphate	n.d.	6.01 (3.05%)	7.16 (7.16%)	n.d.	n.d.	n.d.
Hydroxytyrosol methyl-sulphate	n.d.	9.32 (4.66%)	6.18 (6.18%)	n.d.	n.d.	n.d.
Total metabolism hydroxytyrosol	*10.7%*	*22.1%*	*31.9%*	*0%*	*14.9%*	*0%*
Tyrosol	67.2	94.9	26.8	8.07	29.9	9.41
Tyrosol methyl	n.d.	n.d.	10.8 (10.8%)	n.d.	n.d.	13.7 (13.7%)
Tyrosol sulphate	n.d.	n.d.	9.78 (9.78%)	n.d.	n.d.	n.d.
Total metabolism tyrosol	*0%*	*0%*	*20.6%*	*0%*	*0%*	*13.7%*
p-Coumaric acid	70.4	213	112	1.65	15.6	9.09
p-Coumaric acid disulphate	n.d.	3.04 (1.52%)	n.d.	n.d.	n.d.	n.d.
p-Coumaric acid methyl	n.d.	4.44 (2.22%)	n.d.	n.d.	n.d.	n.d.
Total metabolism p-coumaric acid	*0%*	*3.74%*	*0%*	*0%*	*0%*	*0%*
Pinoresinol	74.32	167	31.7	1.80	15.2	12.3
Pinoresinol sulphate	2.28 (3.06%)	44.3 (22.2%)	20.5 (20.5%)	n.d.	5.48 (2.74%)	3.67 (3.67%)
Pinoresinol glucuronide	n.d.	12.18 (6.09%)	10.04 (10.0%)	n.d.	9.37 (4.69%)	14.9 (14.9%)
Total metabolism pinoresinol	*3.06%*	*28.3%*	*30.5%*	*0%*	*7.43%*	*18.6%*
Luteolin	34.1	31.2	9.54	n.d.	6.10	8.38
Luteolin glucuronide	n.d.	8.96 (4.48%)	8.64 (8.64%)	n.d.	6.37 (3.19%)	6.83 (6.83%)
Luteolin methyl-glucuronide	n.d.	8.54 (4.27%)	10.2 (10.2%)	n.d.	15.5 (7.74%)	7.31 (7.31%)
Luteolin methyl	14.6 (18.3%)	21.6 (10.7%)	11.1 (11.1%)	0.65	7.03 (3.52%)	8.01 (8.01%)
Total metabolism luteolin	*18.3%*	*19.5%*	*29.9%*	*0.65%*	*14.5%*	*22.2%*

[a] Amount in 2 ml cell culture media at 40 μM = 80 nmol.
[b] Amount in 2 ml cell culture media at 100 μM = 200 nmol.
[c] Amount in 2 ml cell culture media at 50 μM = 100 nmol.

Table 4
Transport profile of individual phenol metabolites in CaCo-2/TC7 cell monolayers after different incubation periods (1, 6 and 24 h). A '–' indicates not detected while the number of ' + ' indicates the relative transport rate (+, relatively slow; ++, relatively fast) for phenols and their metabolites in the apical, cellular and basolateral compartments after apical loading of the phenol at 100 μM.

Phenols and metabolites	1 h			6 h			24 h		
	Apical	Cellular	Basolateral	Apical	Cellular	Basolateral	Apical	Cellular	Basolateral
Hydroxytyrosol	++	–	–	++	–	++	+	+	–
Hydroxytyrosol methyl	–	–	–	+	+	+	–	–	++
Hydroxytyrosol sulphate	–	–	–	+	–	++	–	–	++
Hydroxytyrosol methyl- sulphate	–	–	–	–	–	+	–	-	++
Tyrosol	++	+	+	+	+	++	+	–	++
Tyrosol methyl	–	–	–	+	–	–	–	–	+
Tyrosol sulphate	–	–	–	+	–	–	–	–	++
Coumaric acid	++	+	+	++	+	+	++	+	++
Coumaric acid disulphate	+	–	–	+	–	–	–	–	+
Coumaric acid methyl	–	–	–	+	–	+	+	–	+
Pinoresinol	++	+	+	++	+	++	+	+	++
Pinoresinol sulphate	+	+	+	+	+	++	++	+	++
Pinoresinol glucuronide	+	+	+	+	+	+	–	–	++
Luteolin	++	–	+	+	–	+	+	–	+
Luteolin glucuronide	–	–	–	–	–	–	+	–	+
Luteolin methyl-glucuronide	–	–	–	+	–	–	+	–	–
Luteolin methyl	+	+	+	+	+	+	+	+	+

used in the previous study by Manna et al. (2000). Incubation of Caco-2/TC7 cells with tyrosol resulted in slow conjugation; the methyl and sulphate conjugates were only quantifiable after 24 h of incubation showing similar metabolism yields to hydroxytyrosol. Similarly *p*-coumaric acid conjugate production was observed only when the initial concentration of the substrate was 100 μM, indicating a slow rate of conjugate production. At initial substrate concentrations of 40 and 50 μM, no conjugation was observed, regardless of the period of incubation. This slow conjugation of olive oil phenolics by CaCo-2/TC7 cells is in contrast to the previously reported rapid and efficient conjugation of flavonoids such as flavonols in this model system (Barrington et al., 2009).

While the absorption and metabolism of hydroxytyrosol, phenolic acids and flavonoids have been quite extensively studied, the metabolism of lignans has not been reported in any detail. When Caco-2/TC7 monolayers were incubated with pinoresinol over 24 h, the highest concentrations of conjugates were observed at 100 μM (6 h) and 50 μM (24 h) (Table 3). A major metabolite, the sulphate derivative, was observed at highest concentrations after 6 and 24 h of incubation. Pinoresinol glucuronide was also detected, but its contribution to total conjugate levels was low (approximately 6–10%). Metabolism of the luteolin was more rapid than the rest of the phenols considered in this study, and resulted mainly in the formation of the methyl conjugate, independent of the incubation time. However, we could only detect the conjugation of luteolin to form glucuronide and methyl-glucuronide conjugates after the longest incubation times, the concentration of which remained stable in the medium up to 24 h.

3.4. Transport of phenols in the Caco-2/TC7 model of the small intestine

The mechanism of absorption of virgin olive oil phenols is unclear despite the numerous studies reported over the last few years. The different polarity of oleuropein and ligstroside aglycones, tyrosol, hydroxytyrosol, flavonoids and lignans probably results in different mechanisms of absorption (Vissers, Zock, & Katan, 2004). Some studies suggested that the oleuropein and ligstroside aglycones (hydroxytyrosol and tyrosol esterified with elenolic acid) may be hydrolysed in the gastrointestinal tract (Visioli et al., 2003; Vissers et al., 2004), after which the transport of the resulting polar phenols, tyrosol and hydroxytyrosol, might occur *via* passive diffusion (Manna et al., 2000). Other postprandial studies provided evidence that the olive oil phenolic compounds undergo extremely extensive first-pass intestinal/hepatic metabolism in the body, and glucuronide, sulphate and methyl conjugates of hydroxytyrosol and tyrosol are the predominant forms in plasma and urine (Covas et al., 2006; De la Torre-Carbot et al., 2007). Both these reports concluded that the phenolic compounds of virgin olive oil could modulate the oxidative/antioxidative balance in human plasma, in an oxidative stress situation (e.g., the postprandial oxidative stress promoted by lipid-rich diets), with oral doses of olive oil greater than 25 ml. The fact that phenolic compounds from virgin olive oil are bioavailable in humans, even at low doses (22 g per day), supports their potential for a protective role (Marrugat et al., 2004).

However, there is little research focusing on the transport of individual phenol conjugates. Results of the metabolism experiments in the present study showed that all of the phenols were conjugated to different degrees in the Caco-2/TC7 cell culture model of the small intestine. In order to fully understand the absorption of phenols, it is important to understand how conjugation affects the efflux of phenol conjugates from inside the enterocytes. Therefore, the efflux of hydroxytyrosol, tyrosol, *p*-coumaric acid, pinoresinol and luteolin conjugates from clonal Caco-2/TC7 cells was investigated, with specific reference to the presence of the native forms and their metabolites in the apical, cellular and basolateral compartments after different incubation periods.

The transport rate data for phenols and their metabolites to the apical, cellular, and basolateral compartments after apical loading of the phenol at 100 μM is shown in Table 4. In general apical loading of individual phenols resulted in time-dependent efflux of different conjugates. After 1 h of incubation, the native forms of tyrosol, *p*-coumaric acid, pinoresinol and luteolin were detected in the basolateral compartment as well as in the apical and cellular compartments. Similarly a basolaterally favoured efflux was observed for the conjugates of pinoresinol, probably as a consequence of the efficient metabolism of these phenols in the CaCo-2/TC7 model. When the incubation time was increased to 6 h, hydroxytyrosol and pinoresinol and their conjugated forms also showed significant basolateral transport. All the phenols included in the study and their metabolites showed preferential apical to basolateral transport after 24 h of incubation.

4. Conclusion

Limited metabolism of olive oil phenolics was observed using Caco-2/Tc7 cells as a model of the human intestinal epithelium. Although all the phase II enzymes required (methyltransferase, sulpho-transferase and uridine diphosphate glucuronosyltransferase) have been shown to be present in Caco-2 cells, in this study the methylated conjugates were the major metabolites detected. Since it has been reported that sulphate and glucuronide conjugates are found in the plasma and urine of human subjects fed olive oil phenolics, it is likely that these are products of hepatic metabolism. Also, we have shown that there was extensive transport of the parent aglycones and their conjugates to the basolateral side.

Acknowledgements

This work was supported by the Spanish Ministry of Education and Science (project AGL2005-07881-C02-01). Aranzazu Soler is supported by FI2002 program from the Catalan Government (Interdepartmental Commission for Research and Technological Innovation). We thank the Biotechnology and Biological Sciences Research Council (UK) for funding (to PAK, CSMF and SS).

References

Artajo, L. S., Romero, M. P., Morelló, J. R., & Motilva, M. J. (2006). Enrichment of refined olive oil with phenolic compounds: Evaluation of their antioxidant activity and their effect on the bitter index. *Journal of Agricultural and Food Chemistry, 54*(16), 6079–6088.

Barrington, R., Williamson, G., Bennett, R. N., Davis, B. D., Brodbelt, J. S., & Kroon, P. A. (2009). Absorption, conjugation and efflux of the flavonoids, kaempferol and galangin, using the intestinal CaCo-2/TC7 cell model. *Journal of Functional Foods, 1*, 74–97.

Beauchamp, G. K., Keast, R. S. J., Morel, D., Lin, J., Pika, J., Han, Q., et al. (2005). Ibuprofen-like activity in extra-virgin olive oil. *Nature, 437*(7055), 45–46.

Bendini, A., Cerretani, L., Carrasco-Pancorbo, A., Gómez-Caravaca, A. M., Segura-Carretero, A., Fernández-Gutiérrez, A., et al. (2007). Phenolic molecules in virgin olive oils: A survey of their sensory properties, health effects, antioxidant activity and analytical methods. An overview of the last decade. *Molecules, 12*(8), 1679–1719.

Carluccio, M. A., Siculella, L., Ancora, M. A., Massaro, M., Scoditti, E., Storelli, C., et al. (2003). Olive oil and red wine antioxidant polyphenols inhibit endothelial activation: Antiatherogenic properties of Mediterranean diet phytochemicals. *Arteriosclerosis, Thrombosis, and Vascular Biology, 23*(4), 622–629.

Chantret, I., Rodolosse, A., Barbat, A., Dussaulx, E., Brot-Laroche, E., Zweibaum, A., et al. (1994). Differential expression of sucrase-isomaltase in clones isolated from early and late passages of the cell line Caco-2: Evidence for glucose-dependent negative regulation. *Journal of Cell Science, 107*(1), 213–225.

Covas, M. I., Ruiz-Gutiérrez, V., De La Torre, R., Kafatos, A., Lamuela-Raventós, R. M., Osada, J., et al. (2006). Minor components of olive oil: Evidence to date of health benefits in humans. *Nutrition Reviews, 64*(10 Suppl. 1), S20–S30.

De la Torre-Carbot, K., Chávez-Servín, J. L., Jaúregui, O., Castellote, A. I., Lamuela-Raventós, R. M., Fitó, M., et al. (2007). Presence of virgin olive oil phenolic metabolites in human low density lipoprotein fraction: Determination by high-performance liquid chromatography-electrospray ionization tandem mass spectrometry. *Analytica Chimica Acta, 583*(2), 402–410.

Esti, M., Contini, M., Moneta, E., & Sinesio, F. (2009). Phenolics compounds and temporal perception of bitterness and pungency in extra-virgin olive oils: Changes occurring throughout storage. *Food Chemistry, 113*(4), 1095–1100.

Fitó, M., Covas, M. I., Lamuela-Raventós, R. M., Vila, J., Torrents, J., De La Torre, C., et al. (2000). Protective effect of olive oil and its phenolic compounds against low density lipoprotein oxidation. *Lipids, 35*(6), 633–638.

Gil-Izquierdo, A., Zafrilla, P., & Tomás-Barberán, F. A. (2002). An in vitro method to simulate phenolic compound release from the food matrix in the gastrointestinal tract. *European Food Research and Technology, 214*(2), 155–159.

Manna, C., Galletti, P., Misto, G., Cucciola, V., ĎAngelo, S., & Zappia, V. (2000). Transport mechanism and metabolism of olive oil hydroxytyrosol in Caco-2 cells. *FEBS Letters, 470*(3), 341–344.

Marrugat, J., Covas, M. I., Fitó, M., Schröder, H., Miró-Casas, E., Gimeno, E., et al.The members of the SOLOS Investigators. (2004). Effects of differing phenolic content in dietary olive oils on lipids and LDL oxidation. A randomized controlled trial. *European Journal of Nutrition, 43*(3), 140–147.

Masella, R., Varì, R., D'Archivio, M., Di Benedetto, R., Matarrese, P., Malorni, W., et al. (2004). Extra virgin olive oil biophenols inhibit cell-mediated oxidation of LDL by increasing the mRNA transcription of glutathione-related enzymes. *Journal of Nutrition, 134*(4), 785–791.

Massaro, M., Basta, G., Lazzerini, G., Carluccio, M. A., Bosetti, F., Solaini, G., et al. (2002). Quenching of intracellular ROS generation as a mechanism for oleate-induced reduction of endothelial activation in early atherogenesis. *Thrombosis and Haemostasis, 88*(2), 335–344.

Miró-Casas, E., Covas, M. I., Farré, M., Fitò, M., Ortuño, J., Weinbrenner, T., et al. (2003). Hydroxytyrosol disposition in humans. *Clinical Chemistry, 49*(6), 945–952.

Morelló, J. R., Motilva, M. J., Tovar, M. J., & Romero, M. P. (2004). Changes in commercial virgin olive oil (cv. Arbequina) during storage, with special emphasis on the phenolic fraction. *Food Chemistry, 85*(3), 357–364.

Moreno, J. J. (2003). Effect of olive oil minor components on oxidative stress and arachidonic acid mobilization and metabolism by macrophages RAW 264.7. *Free Radical Biology and Medicine, 35*(9), 1073–1081.

Owen, R. W., Giacosa, A., Hull, W. E., Haubner, R., Würtele, G., Spiegelhalder, B., et al. (2000). Olive-oil consumption and health: The possible role of antioxidants. *Lancet Oncology, 1*(2), 107–112.

Owen, R. W., Haubner, R., Wurtele, G., Hull, W. E., Spiegelhalder, B., & Bartsch, H. (2004). Olives and olive oil in cancer prevention. *European Journal of Cancer Prevention, 13*(4), 319–326.

Petroni, A., Blasevich, M., Salami, M., Papini, N., Montedoro, G. F., & Galli, C. (1995). Inhibition of platelet aggregation and eicosanoid production by phenolic components of olive oil. *Thrombosis Research, 78*(2), 151–160.

Ruano, J., López-Miranda, J., De La Torre, R., Delgado-Lista, J., Fernández, J., Caballero, J., et al. (2007). Intake of phenol-rich virgin olive oil improves the postprandial prothrombotic profile in hypercholesterolemic patients. *American Journal of Clinical Nutrition, 86*(2), 341–346.

Servili, M., Taticchi, A., Esposto, S., Urbani, S., Selvaggini, R., & Montedoro, G. (2008). Influence of the decrease in oxygen during malaxation of olive paste on the composition of volatiles and phenolic compounds in virgin olive oil. *Journal of Agricultural and Food Chemistry, 56*(21), 10048–10055.

Suárez, M., Macià, A., Romero, M. P., & Motilva, M. J. (2008). Improved liquid chromatography tandem mass spectrometry method for the determination of phenolic compounds in virgin olive oil. *Journal of Chromatography A, 1214*(1–2), 90–99.

Tuck, K. L., Freeman, M. P., Hayball, P. J., Stretch, G. L., & Stupans, I. (2001). The in vivo fate of hydroxytyrosol and tyrosol, antioxidant phenolic constituents of olive oil, after intravenous and oral dosing of labelled compounds to rats. *Journal of Nutrition, 131*(7), 1993–1996.

Visioli, F., Galli, C., Bornet, F., Mattei, A., Patelli, R., Galli, G., et al. (2000). Olive oil phenolics are dose-dependently absorbed in humans. *FEBS Letters, 131*(7), 159–160.

Visioli, F., Galli, C., Grande, S., Colonnelli, K., Patelli, C., Galli, G., et al. (2003). Hydroxytyrosol excretion differs between rats and humans and depends on the vehicle of administration. *Journal of Nutrition, 133*(8), 2612–2615.

Vissers, M. N., Zock, P. L., & Katan, M. B. (2004). Bioavailability and antioxidant effects of olive oil in humans: A review. *European Journal of Clinical Nutrition, 58*(8), 955–965.